American Scientific Research Journal for Engineering, Technology, and Sciences (ASRJETS)
ISSN (Print) 2313-4410, ISSN (Online) 2313-4402

http://asrjetsjournal.org/

Design and Control of High Altitude Platform for Communication and Navigation Purpose

Rehan Rasheed Khan[a*], Dr. Umer Iqbal Bhatti[b]

[a,b]*Aeronautics and Astronautics, Institute of Space technology, Islamabad, Pakistan.*
[a]*Email: Rehan.khan360@outlook.com*
[b]*Email: uiqbal3@gmail.com*

Abstract

The high altitude platform is designed for navigation and communication purpose. This work focuses on the design and dynamic model of airship that can operate at a height of twenty kilometers above sea level. Significant target of this paper is to propose a coordinating system which can remotely pilot and also has an option of autopilot with auto station keeping. The various control techniques are presented in order to achieve the level flight. First a comprehensive physical and mathematical nonlinear model of the airship is presented and then linearizes it by the means of linearization principles. After that, model based control technique such as Linear Feedback Control (LFC), Linear Quadratic Regulator (LQR) and proportional, integral and differential (PID) control are used to achieve level flight of the airship which give robustness against climatic and outer turbulences. With a specific end goal to represent the model based control strategies. The level flight has been accomplished successfully and has been validated by utilizing Simulink and Flight gear Simulators. The outcomes show that the proposed procedures give soundness, better execution and prudent control endeavors. At the end of the thesis, a comparison is reported to show the performance of the proposed controllers.

Keywords: Airship; Aerospace; Control; Dynamics; Design.

1. Introduction

On the basis of physical structure, the airships arranged in three different types. The "Inflexible Airships", "Semi Unbending Airships" and "Non-Unbending Airships". In recent times, there are further recommendations to build such vehicles which are based on aerostatic elevation standards.

---

* Corresponding author.

However not much depending upon streamlined lift for complete payload limit. These creative vehicle ideas have gotten to be referred to blandly as "hybrid airships". The airship load is primarily relatives to the dimensions. The large volume airship means the more capacity for cargo, although larger dimensions causes some problems in airships such as infrastructure and financially cost more, needs more construction time, required more maintenance beside these they offer unique services and bulky transportation features also the large size mean more comfort for passengers. In recent time, use of hydrogen gas substitute and replaced by the Helium gas. High altitude platform has various advantages such as, it can be used as alternate to satellite system when arrange in constellations to cover a required area or globe, by this it can fulfill the need of communication without depending on the satellite system. As Pakistan do not have its own global satellite system for navigation and communication like America have GPS system and china have beiDou And Russia have its own satellite system for navigation GLONASS. Communication and navigation via airship high altitude platform is a cost effective solution compared to satellite system that others are using.

The most important factor is data security because when we communicate via other's satellite system they can record or keep track of our personal information. As for military communication and navigation we do not have to rely on others. The research work second part is concerned with the airship lateral directional control laws development in turbulence and steady airflow. The airship envelope and a four empennage configuration flight dynamics models (FDM) implemented and discussed which is based on mathematical model of a six-degrees-of-freedom (6DoF) [15,12,16]. In every case, the subsequent system; the airship prototype provided with an electric engine without ballonets and ballast system.

The fixed center of gravity (CG), could be considered as characterized an airframe. By these assumptions, developed airship flight dynamics models (FDM) that presented a body frame having its origin which can be imagined to positioned at the center of volume (CV) but with center of mass, that showed the best practice of ballasted airships [12,16]. Another assumption for airship FDM that the inertia of airship have not included the added mass effects, but moments occurring in accelerated flight and modelled as outside forces. The propulsion effects on aerodynamics have introduced by considering the tail efficiency increment as a result of arrangement of propeller [17].

The core objective to design control system of a platform is station keeping and if needed it can be cruise to change its position or location along with its altitude. The achievement of main objective satisfying the rolling moment control system that decreases the high-frequency sinusoidal motions of an airship and lateral-directional control system development with gusts and turbulence. Approaches to design Control system introduced to bring down the yawing moments, pitching moments, rolling moments which are undesired effect and controlled by elevator deflections and rudder deflection only. According to the pole placement, control system in turbulence air has been designed.

The proportional, integral and differential (PID) gain methods and linear quadratic regulator (LQR) methods is also used. Requirement is to reduce the spending of energy motivated the selection of an optimal control design

technique required to operate the control surfaces.

2. Airship mathematical model

Airship envelope design is based mainly on mathematical modelling and drag estimations which ensures required buoyant lift. As a starting point, the necessary lifting force is converted to an approximate volume using the buoyancy Equation Fundamental aerodynamic modelling are then used to form a computer model, from which the basic design parameters can also be obtained. The concept of double ellipsoids was used for contour design, as it minimizes drag, increases aerodynamic lift and ensures minimum structural loading. Theoretically, a sphere is the best design option with maximum volume to area ratio and hence minimum surface friction drag, but as the fluid moves around the sphere, it forms wake therefore there is pressure symmetry between front and rear of the airship. One technique is to prevent flow separation at the aft of spherical body by attaching a cone. A more suitable solution is to use double ellipsoid to prevent or prolong flow separation to maximum allowable length in order to have minimum drag.

The feasibility study also includes numerical analysis of airships designs. As part of this research, data was collected with regard to specifications of different airships. These specifications included geometric dimensions, weights and performance values. This data are tabulated and used to perform calculations to obtain specific ratios and graphs. Three main ratios were graphed and analyzed previously by Waleed Ahmed and Sajid-ur-Rehman [18]. These were the empty weight to take-off weight ratio, the length to width ratio and the thrust to weight ratio. These ratios are chosen for specific analysis as they provide information useful in the initial design of the airship [18].

Table 1: Statically Analysis Ratio

Parameter	Ratio
Length to width ratio	3
Thrust to weight ratio	0.3
Empty weight to take-off weight ratio	0.6

a. Envelope Design

A suitable solution is to use double ellipsoid to prevent or prolong flow separation to maximum length in order to have minimum value of drag as shown in figure 1.

After initial volume calculations using the following equations, following data are obtained:

Front of Airship **Back of Airship**

$$\frac{x^2}{a^2}+\frac{y^2}{b^2}=1 \qquad \frac{x^2}{4a^2}+\frac{y^2}{b^2}=1 \qquad 1$$

$$y = \sqrt{b^2 - \frac{x^2 b^2}{a^2}} \qquad y = \sqrt{b^2 - \frac{x^2 b^2}{4a^2}} \qquad \textbf{2}$$

$$V_f = \pi \int_0^a \left(b^2 - \frac{x^2 b^2}{a^2}\right) dx \qquad V_b = \pi \int_0^{4a} \left(b^2 - \frac{x^2 b^2}{4a^2}\right) dx \qquad \textbf{3}$$

The following table 2, presents the summarized the mission scenarios that used in, which is according to the mission to navigate the platform over a desired section of the earth for communication that is above land area of Pakistan, latitude and longitude is 30° 00'N and 70° 00'E

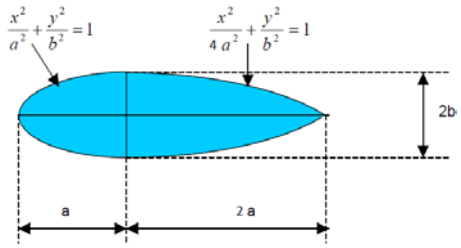

Figure 1: Preliminary Envelop Design [18]

Table 2: Mission Scenario

	Metric
Altitude	20 km
Total mass including Payload	50 kg
Nominal airspeed	18 m/s
Maximum airspeed	46 m/s

The prototype airship framework focus in this thesis comprises of an axisymmetric, tail balances for stability purposes and teardrop-modeled frame with a hanging gondola [20]. The aim of this analysis, to demonstrate the frame as two parts of symmetric ellipsoid hub. Each ellipsoid has unlike semi-major axes-a1 and semi-major axes a2 and has similar semi-minor axis-b, as shown in figure 2.

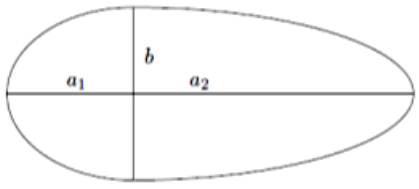

Figure 2: Ellipsoidal Configuration [18]

As indicated in the above figure 2, it is a 2-D perspective model of an ellipsoid airship. Airship ellipsoid geometry is achieve by use of ratios discussed in table 1 and it has been utilized to develop the practical design of airships. The ellipsoid design is consequently utilized as a part of this thesis, as it catches crucial airships aerodynamic attributes while encouraging the model improvement mathematically and scientifically. The initial phase is to outline the procedure to measure the size and structure. The airship's frame volume characterize the buoyant lift ability and it also decides the maximum achievable height. To build up a relationship between gas densities, volume and mass. The airship produced upward buoyancy force which is equivalent to dislodged air heaviness. This force is commonly referred as "gross lift" and characterized as:

$$L_G = V_N \rho_A g \quad \textbf{4}$$

Where the dislocated air net volume is V_N, air density is ρ_A, and gravity is denoted by g. by subtracting lifting gas (Helium) heaviness, we will get the L_N which is the net lift. Noticing that the dislodged air volume is equivalent to the Helium gas volume, so the mathematical statement for the net lift L_N is written as

$$L_N = V_N (\rho_A - \rho_H) g \quad \textbf{5}$$

The mathematical statement provides lift accessible measure to balance the air-vehicle structure and payload heaviness. The air and Helium thickness both shift with height. Expecting that these two gasses have same temperature and pressure, and with an elevation their densities change negatively. In spite of the fact that a slight pressure differential is necessary for the system to rise to a certain height, for this analysis it is better to discard it as is too minor. As the airship rises, the atmospheric density declines along with the thickness of Helium. The airship governs given essential aerostatic law and accepting a classic model of teardrop shape for the structure. It is feasible for picking measurement arrangements which give a suitable volume for the pressure airship working at a height of 20 km. We first utilize the expression in equation 6, since σ_p=0.0061 ρ_{Ao}=1.275 kg/m^3, ρ_{Ho}=0.176 kg/m^3, total mass is 50 kg.

$$V_{max} = \frac{m_{total}}{\sigma_p (\rho_{Ao} - \rho_{Ho})} = 691.71\ m^3 \quad \textbf{6}$$

This mathematical statement decides the volume required for the airship body based upon the density proportion and the airship structure and payload mass. Hence, the airship mass also dependent on the required volume, it turns into an outline test to amplify the volume while minimizing the basic mass. Give a chance to separate the complete airship mass as in equation 7 shown below:

$$m_{total} = m_f + m_s + m_p \quad \textbf{7}$$

Where the outside fabric mass is m_f, the airship structure and every supporting framework mass is m_s and the payload mass is m_p. The outside fabric mass is relative to the surface area by the fabric density ρ_f.

$$m_f = \rho_f S \quad \textbf{8}$$

The maximum distance across of the body is characterized as D = 2b, while the length is L = a1 + a2 and k presents the length fraction, characterized as shown in equation 9.

$$k = \frac{a2}{a1} = 3 \quad \textbf{9}$$

Since L/D= 3 and L=4a1 therefore volume for ellipsoidal is:

$$V_{max} = \frac{\left(\frac{4}{3}\pi b^2 a_1\right)}{2} + \frac{\left(\frac{4}{3}\pi b^2 a_2\right)}{2} \quad \textbf{10}$$

Since L=a1+3a1=4a1 therefore L/D= (4a1/2b) =3 so a1=6b/4 and new formula of volume is:

$$V_{max} = \frac{\left(\frac{4}{3}\pi b^2 \frac{6b}{4}\right)}{2} + \frac{\left(\frac{4}{3}\pi b^2 \frac{24b}{4}\right)}{2} \quad \textbf{11}$$

$$V_{max} = \frac{(2\pi b^3)}{2} + \frac{(8\pi b^3)}{2} \quad \textbf{12}$$

$$V_{max} = 5\pi b^3 = 691.71 m^3 \quad \textbf{13}$$

Therefore:

$$b = \sqrt[3]{\frac{691.71}{5\pi}} = 3.531\ m \quad \textbf{14}$$

Therefore a1=5.3 and a2=15.9

With a specific end goal the limitation of k > 1 is forced to keep up the teardrop shape. An illustration geometry is demonstrated, with L = 21.2 m; k = 3 and D = 7.06 m. It takes after that a2 = 15.9 and a1 = 5.3.

b. Airship Power Requirement

The drive system required power with proficiency η_p to apply push T at speed U is given as:

$$P_{req} = \frac{TU}{\eta_p} \quad \textbf{15}$$

To look after harmony, the thrust must be equivalent to the drag.

During the day time, solar cells produce electrical power. This fluctuates from zero at morning to at maximum in the early afternoon, and then turns to zero again at night [21]. The expression is written as:

$$P_{gen}(t) = SRI_{sol}(t)\eta_{sc} \quad \textbf{16}$$

Where the complete structure surface area is S, the surface area secured with sun oriented cells is denoted by R, the sunlight based irradiance is represented as I_{sol} and the sun powered cell effectiveness is $\eta_{sc} < 1$. The

calculations did not consider the way that the cell typically points in a particular direction or in the direction of sunlight. This may be represented by changing η_{sc} so it mirrors the normal productivity, along with directional impacts.

By integrating P_{req} from t = 0 to 24 hours, aggregates power energy required over a 24 hour period can be find. The expression for substituting the drag for the thrust and utilizing normal speed U is written as in equation 17 [21].

$$P_{req} = \left(\frac{\rho \underline{U} S C_D}{2\eta_p} + P_0\right) t_{day} \quad \textbf{17}$$

Where the payload need power P_0 (1.5 kW) and the number of seconds when sunlight is present is t_{day}. With the incorporation of P_{req} from dawn t_{sr} to dusk $t_{ss,}$ the aggregate vitality created over a 24 hour period can be find. The sunlight diversity based irradiance may be approximated as a sinusoidal curve from 0 to 180 degree as in equation 18 [21].

$$P_{gen} = \frac{2}{\pi} SR\eta_{sc} E_{max}(t_{ss} - t_{sr}) \quad \textbf{18}$$

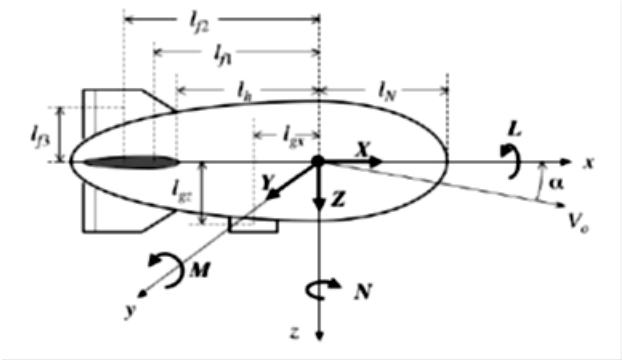

Figure 3: Aerodynamic Model [25]

The complete airship geometric setup with gondola and control surfaces is shown in Figure 3[26, 25, 21]. It is shown to be flying at a velocity V_0 speed and at approach α.

The sideslip angle β is characterized as a positive turn about the z-axis, measured from the x-axis. These moments are entitled with L, M, N, and the forces denoted as X, Y, Z.

The moments and forces on the frame are assessed control surfaces from the beginning to the nose. Toward the back of this point, the structure and control surfaces are assessed together [27, 28].

The airship body frame origin is located at the center of volume. The volume center is located on the x-axis at the point in double-ellipsoid geometry. Where x_{cv} is measured in reverse from the nose.

$$x_{cv} = a_1 + \frac{3}{8}(a_2 - a_1) = 9.275\ m \quad \textbf{19}$$

For an airship, it is a regular practice to express the reference zone as far as the structure volume:

$$A = V^{2/3} = 78.214\ m^2 \quad \textbf{20}$$

As per previous analysis [18] thrust to weight ratio is 0.3 therefore the thrust required is:

$$\frac{THRUST}{WEIGHT} = 0.3$$

$$THRUST = 0.3(WEIGHT) = 147.15\ N \quad \textbf{21}$$

Payload Calculation is:

$$\frac{Empty\ Weight}{Take\ off\ Weight} = 0.6$$

$$Empty\ Weight = 0.6\ Take\ off\ Weight = 30\ kg \quad \textbf{22}$$

Therefore pay load comes out to be 20 kg and we have to design complete structure of the airship within 30 kg.

c. Aerodynamic Data of Airship

Main characteristics of the platform are calculated in previous sections is listed in table 4 and a general flying conditions are assumed according to the mission scenario discussed in previous section are listed in table 3. Aerodynamic data listed in below Tables are representing derivatives at a single sideslip angle and angle of attack as mentioned in Table 3.

Derivatives of varying angle of attack with fixed sideslip angle are calculated for coefficients calculations. All aerodynamic data coefficients is calculated using digital DATCOM software according the characteristics and flying condition.

Table 3: Airship Flying Condition

Flying Condition	
Cruise speed	0.04 Mach
Altitude	20 km
Sideslip angle	1 degree
Angle of attack	2 degree

Table 4: Airship Main Characteristics

Airship	
Envelope volume	691.71 m3
Overall length	21.2 m
Max diameter	7.062 m
Helium purity	0.97
Max speed	46 m/s
Fin surface area	3 m2
Control surface area	1 m2
Vector able propellers	2 units
Nominal thrust per unit	147.15 N
Thrust vectoring range	180
Fin airfoil	NACA 1412

d. Equations of Motion

The conventional study of control and stability needs a scientific model created around the equations of motion [7] [20] [31] [12] [32]. The mathematical model of airship is based on dynamic model of six degree of freedom (6-DOF). Initially, on the basis of the standards the airship equations of motion have been developed that obeys the following assumptions:

- The mass of airship remains constant.
- There is no aero-elastic effects and the airship is perceived as a rigid body.
- Relating to the longitudinal plan the airship is seem symmetric, that belongs to the centers of gravity and buoyancy of airship.
- The two independent thrust vector propellers and control surfaces are provided with airship.
- The equilibrium flight of airship is rectilinear.
- It is supposed that no effects of turbulence exists and the model is steady air.

$$\frac{dQ}{dt} = \sum F$$

$$\frac{dK}{dt} = \sum M \qquad \textbf{23}$$

At the airship, the body axes *CV* (Figure 3) are conventionally centered that denotes the system immovable point. Suppose the symmetry problem, the gravity and buoyancy midpoint will be zero $a_y = b_y = 0$, also the inertia products will be $I_{xy} = I_{yz} = 0$ zero too. As the above stated conventions, the general dynamic airship

equation 23 will be put in writing as shown, then the linearized motion equations will developed.

In supplement to the common term of aerodynamics, in addition to the static buoyancy and inertial terms the airship motion equations will also consist of moment terms and significant force; as the airship included the air mass dislodged in acceleration. This air mass offers rise to inertia effects and virtual mass that formally stated as equivalent to the acceleration derivatives of aerodynamics. The added inertia moments and mass introduced in the following expressions:

i. Longitudinal Equations

The following section stated the linearized longitudinal motion equations for airship:

$$m_x\dot{u} + (ma_z - \dot{X}_{\dot{q}})\dot{q} = X_e - m_z W_e q + \dot{X}_u u + \dot{X}_w w + \dot{X}_q q + \dot{X}_\delta(\delta_e + \delta_r) + T_s\cos\mu_s + T_p\cos\mu_p - (mg - B)(\sin\theta_e + \Theta\cos\theta_e)$$

$$m_z\dot{w} - (ma_x - \dot{Z}_{\dot{q}})\dot{q} = Z_e + m_x U_e q + \dot{Z}_u u + \dot{Z}_w w + \dot{Z}_q q + \dot{Z}_\delta\delta_e - T_s\sin\mu_s - T_p\sin\mu_p + (mg - B)(\cos\theta_e - \Theta\sin\theta_e)$$

$$J_y\dot{q} - (ma_x - \dot{M}_{\dot{w}})\dot{w} + (ma_z - \dot{M}_{\dot{u}})\dot{u} = M_e - (ma_x U_e + ma_z W_e)q + \dot{M}_u u + \dot{M}_w w + \dot{M}_q q + \dot{M}_\delta\delta_e + T_s(d_z\cos\mu_s - d_x\sin\mu_s) + T_p(d_z\cos\mu_p - d_x\sin\mu_p) + (mga_x + Bb_x)(\theta_e\sin\theta_e - \cos\theta_e) - (mga_z + Bb_z)(\sin\theta_e + \Theta\cos\theta_e) \quad \textbf{24}$$

ii. *Equation of Lateral-Directional*

The following equations resulting in developed linearized lateral-directional motion equation of an airship [33,34,20,24,7,35,29]:

$$m_y\dot{v} - (ma_z + \dot{Y}_{\dot{p}})\dot{p} + (ma_x - \dot{Y}_{\dot{r}})\dot{r} = Y_e + \dot{Y}_v v + (\dot{Y}_p + m_z W_e) + (\dot{Y}_r - m_x W_e) + \dot{Y}_\delta\delta_r + (mg - B)\emptyset\cos\theta_e$$

$$J_x\dot{p} - J_{xz}\dot{r} - (ma_z + \dot{L}_{\dot{v}})\dot{v} = L_e + \dot{L}_v v + (\dot{L}_p - m_z W_e)p + (\dot{L}_r + m_z U_e)r + \dot{L}_\delta\delta_r - (mga_z - Bb_z)\emptyset\cos\theta_e$$

$$J_z\dot{p} - J_{xz}\dot{r} - (ma_x + \dot{N}_{\dot{v}})\dot{v} = N_e + \dot{N}_v v + (\dot{N}_p + m_x W_e)p + (\dot{N}_r - m_x U_e)r + \dot{N}_\delta\delta_r - (mga_x - Bb_x)\emptyset\cos\theta_e \quad \textbf{25}$$

The rectilinear flight results as all zeros ($Y_e = L_e = N_e = 0$), when applying the lateral-directional trim conditions. The airship linearized lateral-directional problem in the state space form can be devised as follows:

$$M_{3\times3}\ \dot{x}_{3\times1} = A_{3\times3}\ x_{3\times1} + B_{3\times2}\ u \qquad \textbf{26}$$

3. Airship control

a. Applied Equations of Motion:

Among the goals of the research, one is concern with satisfying the rotational and translational control system achievements in atmosphere, which reduce oscillatory motions of high-frequency and high altitude platform. The platforms' purpose is to build a reliable navigation and communication link. The video and picture acquisition systems are troubled by the oscillatory motion that shows the vehicle payload. The cross configuration is a typical a high altitude platform configuration. With respect to the envelope longitudinal centerline [34,20,7,24,28], due to the *center of gravity* offset, the continuous rolling motions create as unwanted effect from the rudder deflections. The two different modes has developed by feedback control algorithm. The closed-loop, lateral-directional and the high altitude platform control have carried out via acting on the rudders and elevators control that offers combined effect as ailerons. The second mode is longitudinal feedback control which has been carried out by acting throttle, propeller pitch angle and elevator control. In lateral control, rudder and elevator together produces the effect of aileron which in turn greatly affects the roll rate [34,20,7,24,28].

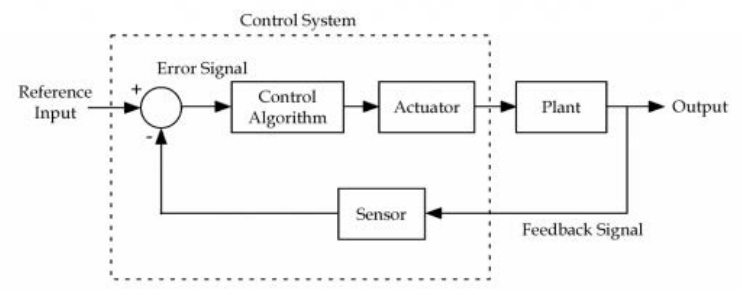

Figure 4: Basic Feedback Control System

From the state-space approach, the closed-loop flight control has succeeded. Linearizing the six degree of freedom (6DoF) model about the reference condition of equilibrium, the state space dynamic system's modeling has carried out.

The lateral and longitudinal equations are decoupled and written in the state space form by using the small disturbance theory of high altitude platform.

The preceding equations $\dot{x} = [\dot{u}, \dot{w}, \dot{q}]^T$ defined as the longitudinal state vector, in which they are as vertical acceleration, forwarded acceleration, and pitch rate are longitudinal state variables.

Lateral state vector defined as $\dot{x} = [\dot{v}, \dot{p}, \dot{r}]^T$, that is side acceleration, roll rate and yaw rate are lateral state variable. In the longitudinal mode there are three inputs throttle, propeller pitch angle and elevator deflection angle therefore the input vector $U = [\tau, \mu, \delta_e]$ is a 1 × 3 matrix.

In the lateral mode there are two inputs rudder and aileron where aileron effect is produced by deflecting both the control surface rudder and elevator, therefore the input vector $U = [\delta_r, \delta_a]$ is a 1 × 2 matrix [21].

b. PID Controller

The practical simplicity and the robust performance of PID controllers in wide range of operating conditions that can be attributed partially, which let engineers to simply use them and in straight forward manner.

The implementation of this sort of controller's need that the three parameters (derivative gain, proportional gain and integral gain) must be determine for given process [23,21,40,41].

Consider the PID controller [42,43]

$$PID(C) = K_P + \frac{K_I}{s} + K_d s \qquad \textbf{27}$$

i. The Robust PID-Controlled System Design

The PID controllers' three coefficients selection is basically a three dimensional space a search problem [43]. The three parameters of PID controllers point in the search space corresponds to different selections.

The different steps response for step input can be produce by choosing different points in the parameter space. For moving in search space on error and trial basis, the PID controller can be determined [40,41,43,43].

The selection of three coefficients is the core difficulty that these do not freely transform into the preferred characteristics of robustness and performance that designer of control system has in his mind. For resolving this problem, numerous procedures and techniques have been proposed.

The integral of time-weighted absolute error (ITAE) performance index and the indices of performance method used is to calculate according to the following optimum coefficients table for the step input. Therefore, three PID coefficients selection is to minimize the ITAE performance index, which produces excellent transient response to step input. Integral of time-weighted absolute error (ITAE), is one of the performance indices that provides the best selectivity of amongst the performance indices.

ITAE's general formula is:

$$ITAE = \int_0^T t|e(t)|\, dt \qquad \textbf{28}$$

The following table shows the optimum coefficients of close loop transfer function based on the ITAE's criterion for a step input.

Table 3: Integral Time-Weighted Absolute Error

Order of system	Characteristic Equation of Close-loop Transfer Function
1st	S + ωn
2nd	S2+1.4ωnS+ωn2
3rd	S3+1.75ωnS2+2.15ωn2S+ωn3
4th	S4+2.1ωn S3+3.4ωn2 S2+2.7ωn3S+ωn4

The design procedure consists of three steps:

- Select the ω_n of the closed loop system by specifying the settling time
- Determine the three coefficients using the appropriate optimum equation and the ω_n of previous step to obtain $G_c(s)$
- Determine a prefilter $G_p(s)$ so that the close loop system transfer function, T(s), does not have any zeros, as required by the ITAE criterion equation.

The airship's PID feedback control angular velocity and rates have been provided by the simple design of control law. The design flight condition has 15m/s nominal airspeed, straight and at target level of 20 km altitude. On the basis of the plant input matrix's analysis for each mode, distinct controllers are created for tailing loops:

Longitudinal Mode:

Axial velocity-to-throttle

Vertical velocity-to-propeller pitch angle

Pitch rate-to-elevator deflection angle

Lateral-Directional Mode:

Side velocity-to-rudder

Yaw rate-to-rudder

Roll rate-to-both rudder and elevator

The controller for each loop is a PID with the transfer function having the form:

$$PID(C) = K_P + \frac{K_I}{s} + \frac{K_d s}{s+1} \quad \textbf{29}$$

The standard PID controller's integral, derivative and proportional gains are directly relating with the K_I, K_P, K_D. By an iterative process, these are already chosen for each loop in which time response and robustness margins evaluated, till the required performance is achieved. 45 degree phase margin and 6 dB gain margin are the standard military robustness preferred requirements that achieved in every loop.

The complete non-linear simulation is conducted with the implementation of controllers at 1 Hz. The 50% damped is supposed to be the perfect actuations and measurements.

The airship is set at 20 km altitude and 15 m/s flying speed along with 2 degree attack angle and 1 degree sideslip. The preferred velocity is 16 m/s with zero degree attack angle and sideslip. The Figure 8 shows time-response. Although the air speed is too away that of the controllers designed, but still provide sound performance. The augmented reply is too faster than of the open loop system, and all actuators work well within their physical limits.

Following results are the closed loop responses of PID controller which shows good stability response over wide range of input and the limiting input of speed is 40 m/s. Separate PID control is applied to all the input-output relationship as discussed above.

Figure 5-7 shown below is the PID response of the control loop of rates. Y-axis represents rate in radians/s and X-axis represent time in seconds. Initially rate is zero but the disturbance is induced by the airship speeds. Elevator and rudder both are used to stabilize the moments of the airship. Roll rate stabilized response achieved in 0.6 seconds, pitch rate in 2 seconds and yaw rate in 10 seconds.

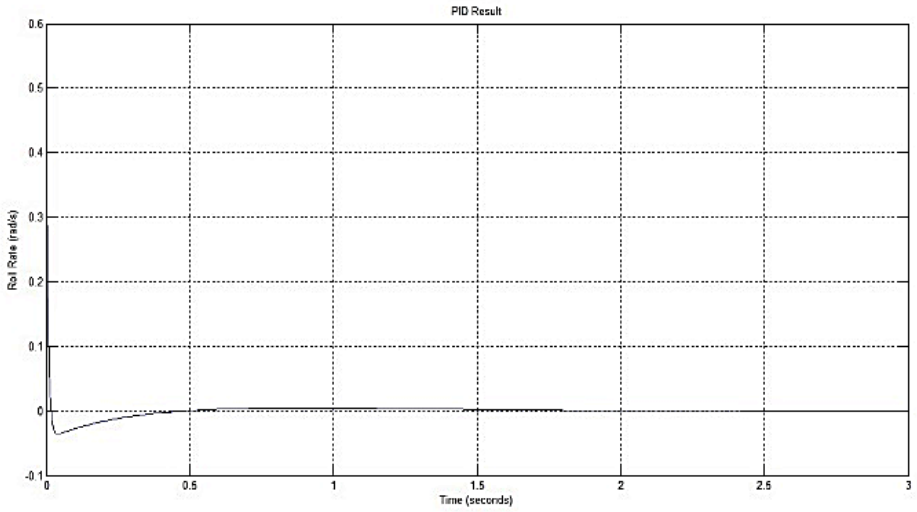

Figure 5: PID Response of Roll Rate (rad/s) Against Time (s)

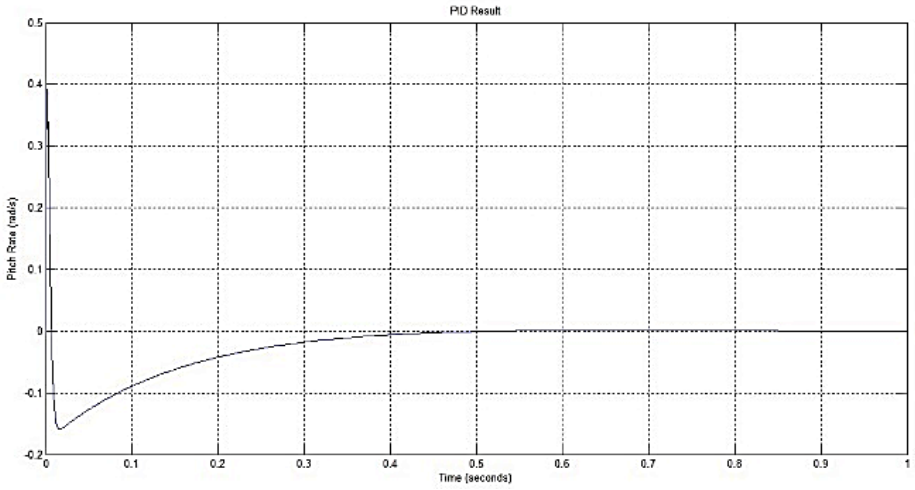

Figure 6: PID Response of Pitch Rate (rad/s) Against Time (s)

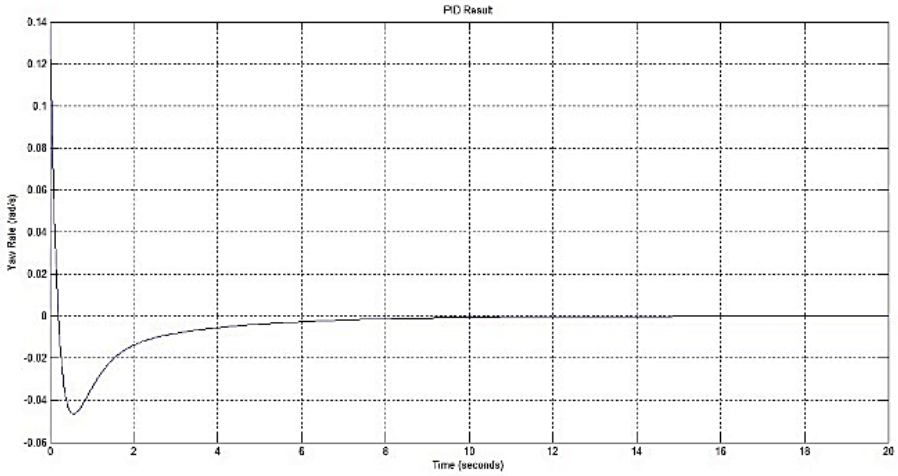

Figure 7: PID Response of Yaw Rate (rad/s) Against Time (s)

c. The Pole Placement Design

Accordingly to the method of pole-placement determined the controller. The information of the poles which assure the system preferred behavior linked with the controller design criteria, like the settling time and overshoot from which the real part of the poles and damping are derived. The closed loop controllers design criteria are set to acquire the preferred response as:

- Overshoot is 5%
- Settling time 5 seconds

$$M_p = 100e^{\left(\frac{-\varepsilon\pi}{\sqrt{1-\varepsilon^2}}\right)} \quad \textbf{30}$$

$$\omega_n = \frac{4.6}{\varepsilon T_s} \quad \textbf{31}$$

$$\sigma = \varepsilon\omega_n \quad \textbf{32}$$

$$\omega_d = \omega_n\sqrt{1-\varepsilon^2} \quad \textbf{33}$$

$$poles = \sigma \pm \omega_d j \quad \textbf{34}$$

$$3^{rd}pole = n\varepsilon\omega_n \quad \textbf{35}$$

Where the overshoot percentage is 'M_p', the coefficient of damping is 'ϵ' zeta, the natural frequency is 'ω_n', the real part of the pole is 'σ' sigma, and the imaginary part of the pole is 'ω_d'.

By the state space linear analysis obtained the controller gains with feedback control laws that presented in the simulation models to compare the closed-loop results with open-loop responses subsequently. So as to avoid deflections i.e. beyond ranges, upon which the control surfaces are not working appropriately, and the simulation model introduced the saturation blocks, and from feedback control laws imposing the upper and lower parameters on input signal. These limits are supposed as −15 and 15 that are the surface deflections upon which the aerodynamics coefficients' maximum absolute values are achieved.

Figure 8 shown below is the pole placement feedback response of rotation rates. Y-axis represents rotation rates in radians/s and X-axis represent time in seconds. Initially rotation rates is zero but the disturbance is induced by the initial airship speeds. Feedback is used to stabilize the airship and it is achieved in 1 seconds.

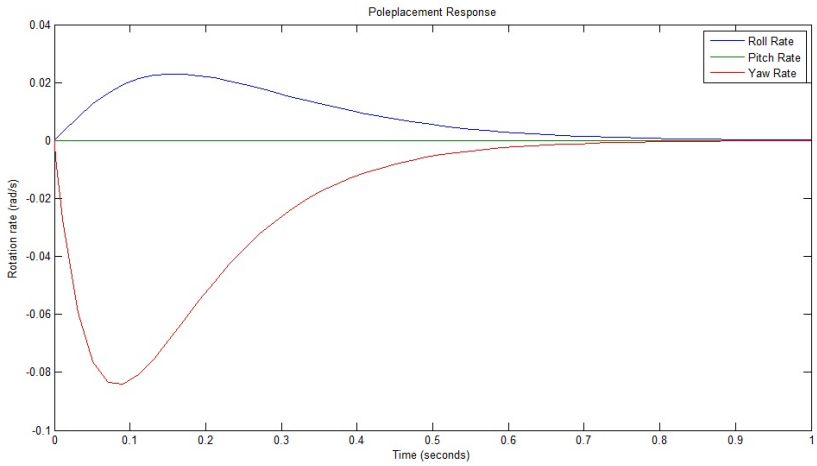

Figure 8: Pole Placement Response of Roll Rate (rad/s) Against Time (s)

d. Linear Quadratic Regulator Control

The performance index *J* can be deduced as energy function that making its small value to keep the closed-loop system's total energy short. Remembering, the x(t) state and u(t) the control input are normally weighed in index *J*, which means that x(t) and u(t) cannot be too big if the value of index *J* is small. While if the index *J* is minimalized so it surely finite. As it is x(t) is an infinite integral which means that x(t) tends to zero as time 't' reaches to infinity. This assure the closed loop system will be stable [47,48].

$$J = \int_0^\infty (x^T Q x + u^T R u) dt \qquad \textbf{36}$$

The two weight matrices Q and R, are *NxN* matrix and *MxM* matrix respectively selected [47]. Depending on how parameters of design are chosen, the closed-loop system will response differently. Generally, to keep J small means picking a larger Q and the state x(t) must be smaller. Contrary, to keep J small means choosing a larger R that the control input u(t) must be smaller. This conclude the greater Q values results in closed-loop system poles matrix A_c= (A-BK) being more left in s-plane, therefore the state decays to zero faster. In contrast, larger R means using the less control efforts, thus the poles are usually slower and resulting the higher state x(t) values.

The Q and R are should be pick up semi-definite positive and definite positive respectively. It implies that the $x^T Qx$ scalar quantity is either positive or zero for each time ''t'' for all x(t) functions, and the $u^T Ru$ scalar quantity is positive for each time "t" for all u(t) values. This make sure that J is defined well. In terms of Eigen values, the Q and R values should be positive. If the diagonal matrices are selected, this means all the Q and R entries should be positive, and with the probability of some zeros are exists on its diagonal, then R is invertible.

The following are the cost matrices assumed as the best trial and error substitution approach for the optimal control formulation:

Longitudinal mode LQR matrix:

$$Q_L = \begin{pmatrix} 1000 & 0 & 0 \\ 0 & 100 & 0 \\ 0 & 0 & 10 \end{pmatrix}$$

$$R_L = \begin{pmatrix} 10 & 0 & 0 \\ 0 & 2 & 0 \\ 0 & 0 & 25 \end{pmatrix}$$

Lateral mode LQR matrix:

$$Q_T = \begin{pmatrix} 100 & 0 & 0 \\ 0 & 10 & 0 \\ 0 & 0 & 1 \end{pmatrix}$$

$$R_T = \begin{pmatrix} 5 & 0 \\ 0 & 0..15 \end{pmatrix}$$

From perspective of the applications, for the lateral-directional regulation's purpose it can be observed that rudder and aileron both are more appropriate to use. The optimal control results are plotted in following figures 5.15 to 5.20 for this strategy, by supposing the exponential decay rate α is equal to 1.1. This certain value originates from the analysis taken in this section, by expression as discussed above.

Figure 9-11 shown below is the LQR feedback response of rotation rates. Y-axis represents rotation rates in

radians/s and X-axis represent time in seconds. Initial condition for all the three rate is zero and LQR Feedback is used to stabilize the atmospheric and environmental disturbances and it is achieved in 0.5 seconds.

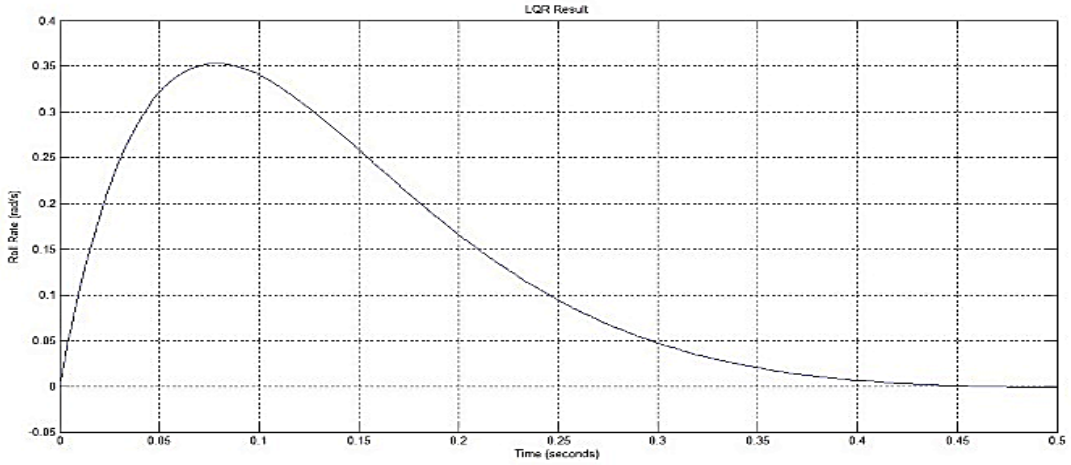

Figure 9: LQR Response of Roll Rate (rad/s) Against Time (s)

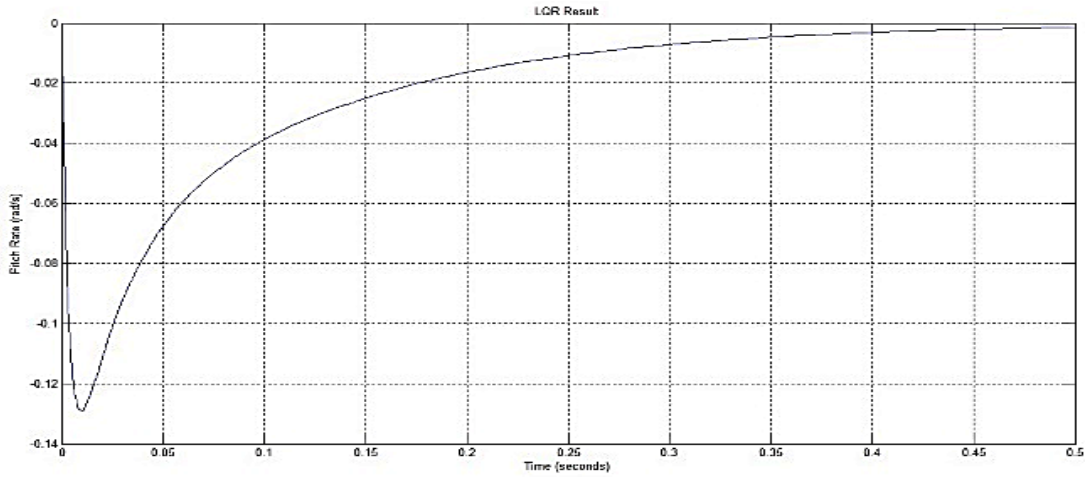

Figure 10: LQR Response of Pitch Rate (rad/s) Against Time (s)

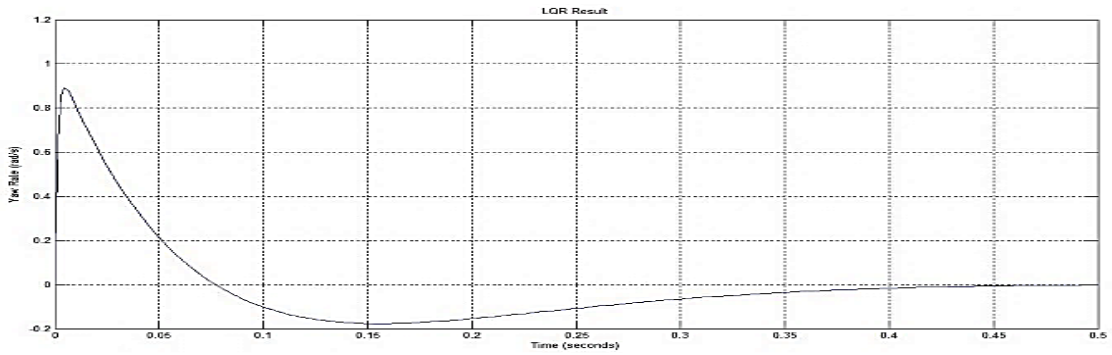

Figure 11: LQR Response of Yaw Rate (rad/s) Against Time (s)

4. FlightGear Results

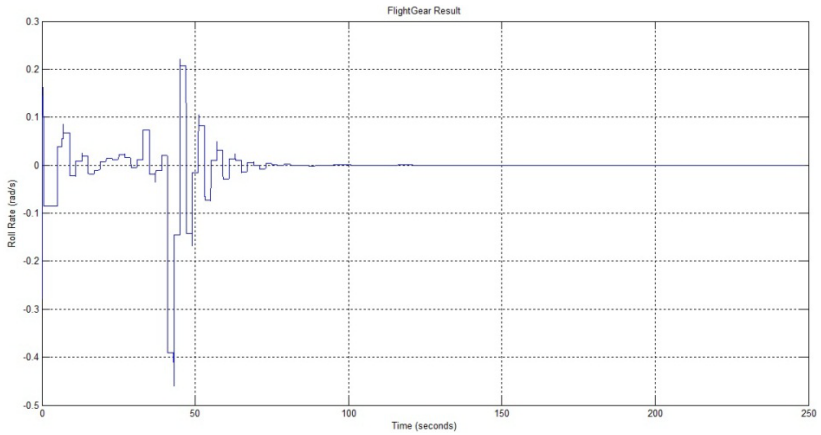

Figure 12: Validation of Rolling Moment by FlightGear rad/s Against Time (s)

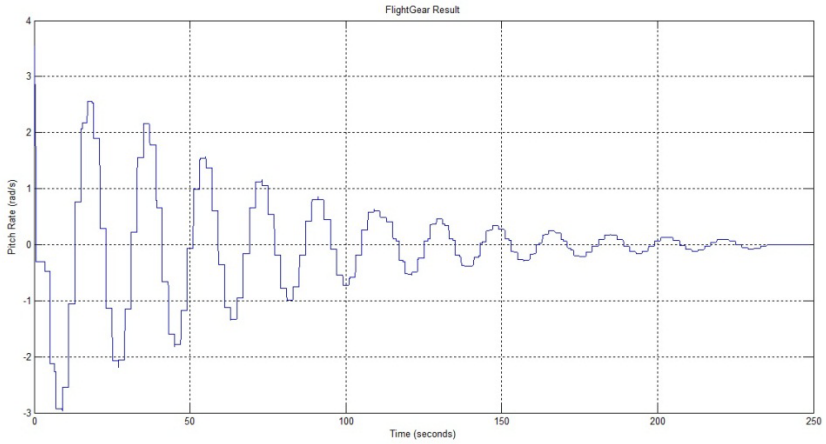

Figure 13: Validation of Pitching Moment by FlightGear rad/s Against Time (s)

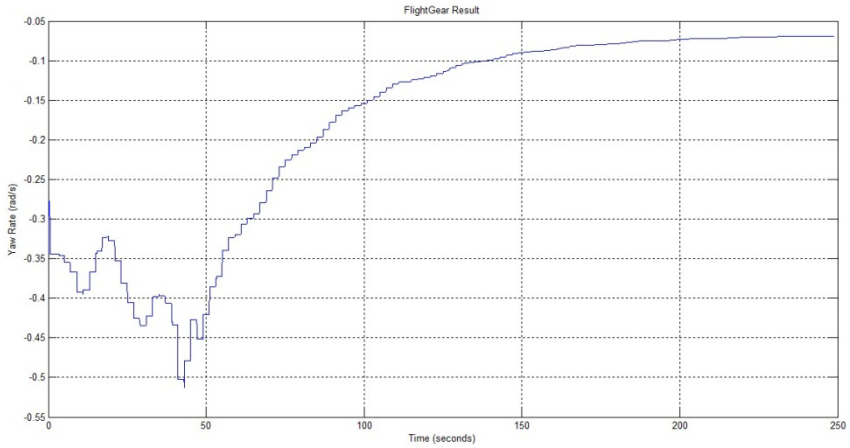

Figure 14: Validation of Yawing Moment by FlightGear rad/s Against Time (s)

Figure 12-14 shown is a validation results using FlightGear software the three rotational moment of airship controlled by the closed loop system by pole-placement method. Y-axis represents rate of rotation in rad/s and X-axis represents time in seconds. Yawing moment is being reduced to zero by control effort in 200 seconds while pitching moment takes 250 seconds and rolling moment is stabilized in 100 seconds.

5. Comparison of results

Table 4: Settling Time Comparison

Settling Time (S)	State Space	FlightGear
Roll moment	1 s	100 s
Pitch moment	1 s	250 s
Yaw moment	1 s	250 s

An only rotation rate is compared since it is a major source of disturbance due to atmosphere and environment. State space is a linear model we can observe that the controller that is designed for that model brings the system to a stable state in predefined required time. On the other hand FlightGear have some nonlinearity therefore the same controller stabilized the system in 100 seconds. FlightGear is a commercially used simulator which have highly nonlinear model and the controller used stabilized the system in 100 seconds.

6. Conclusion

High altitude platform has various advantages such as, it can be used as alternate to satellite system when arrange in constellations to cover a required area or globe, by this it can fulfill the need of communication without depending on the satellite system. As Pakistan do not have its own global satellite system for navigation and communication like America have GPS system and china have beiDou And Russia have its own satellite system for navigation GLONASS. Communication and navigation via airship high altitude platform is a cost effective solution compared to satellite system that others are using. Our contribution in this paper is a design of an airship that can lift a total load of fifty kilogram. Designing a controller and validate its results using state of the art FlightGear model. Also comparing the results of different models using the same controller. The comparison of linear and nonlinear control loop response enable us to design more reliable control system. Hardware can be fabricated in future to practical implementation of the system.

References

[1] "http://www.airships.net/hydrogen-airship-accidents," last date accessed 1\8\2016.

[2] "http://www.airships.net/us-navy-rigid-airships/uss-akron-macon," last date accessed 1\8\2016. .

[3] "http://www.navsource.org/archives/02/99/029904.htm," last date accessed 1\8\2016. .

[4] "http://www.airships.net/hindenburg/disaster," last date accessed 1\8\2016. .

[5] "https://en.wikipedia.org/wiki/Hindenburg_disaster," last date accessed 1\8\2016. .

[6] "http://www.theatlantic.com/photo/2012/05/75-years-since-the-hindenburg-disaster/100292/," last date accessed 1\8\2016. .

[7] M. Acanfora, New Approach and Results on the Stability and control of Airship, UNIVERSITA' DEGLI STUDI DI NAPOLI "FEDERICO II", 2011.

[8] "https://en.wikipedia.org/wiki/Airship," last date accessed 1\8\2016. .

[9] "http://www.worldskycat.com/markets/skypatrol.html," last date accessed 1\8\2016. .

[10] "http://www.lockheedmartin.pk/us/products/integrated-sensor-is-structure.html," last date accessed 1\8\2016. .

[11] F. Goineau and M. V. Cook, "The stability and control characteristics of the neutrally buoyant non-rigid airship, ,," Cranfield Institute of Technology,, no. College of Aeronautics Reports, 1999..

[12] M. V. Cook, K. G.A. and G. J.D, "Stability and Control. by.,," Chap. IV in Airship technology, no. ,Cambridge University Press, , 1999..

[13] E. A. Kulczycki and J. R. Johnson, "The Development of Parameterized Linear Analytical Longitudinal Airship Model," AIAA Guidance, Navigation And Control Conference And Exhibit,, Vols. Honolulu (Hawaii),, no. Paper No.7260, , 2008.

[14] M. V. Cook, " The linearized small perturbation equations of motion for an airship,," College of Aeronautics Reports, WP8, Cranfield Institute of Technology,, 1990..

[15] "J. Rao, Z. Gong, Z. Xie, A Flight Control and Navigation System of a Small Size Unmanned Airship. IEEE International Conference on Mechatronics & Automation, Niagara Falls, Canada, 2005, pp. 1491-1496.".

[16] "S. B. V. Gomes, J. Jr. G. Ramos, Airship Dynamic Modeling for Autonomuos Operation. IEEE International Conference on Robotics & Automation, Leuven, Belgium, 1998, pp. 3462-3467.".

[17] "J. R. Azinheira, E. Paiva, J. J. G. Ramos, S. S. Bueno, M. Bergerman, Extended".

[18] W. Ahmed and S. u. Rehman, "Semi-Rigid Hybrid Airship," Department of Aeronautics and Astronautics , Institute of Space Technology, 2013.

[19] L. KONSTANTINOV, "The Basics of Gas and Heat Airship Theory".

[20] "A. Moutinho, Modeling and Nonlinear Control for Airship Autonomous Flight, PhD Thesis, University of Lisboa, December 2007.".

[21] "Development of an Aerodynamic Model and Control Law Design for a High Altitude Airship," AIAA, 2004.

[22] "H. Lamb, The Inertia Coefficients of an Ellipsoid Moving in Fluid. Aeronautical Research Council Report 623, Aeronautical Research Council, 1918.".

[23] "J. Carvalho, E. de Paiva, J. Azinheira, P. Ferreira, J. Ramos, S. Bueno, M. Bergerman, S. Maeta, L. Mirisola, L. Faria, A. Elfes, Classic and robust PID heading control for an unmanned robotic airship. SIRS'2001 Int. Conf., Toulouse, France, Jul 2001, pp.".

[24] "A. Tewari, Modern Control Design with Matlab and Simulink. John Wiley & Sons Ltd, ISBN 0 471 496790, 2002.".

[25] C. Stockbridge, A. Ceruti and P. Marzocca, "Airship Research and Development in the Areas of Design, Structures, Dynamics and Energy System," Aeronautical and Space Science, 2012.

[26] L.B.TUCKERMAN, "Inertia Factors Of Ellipsoids For Use In Airship Design," NATIONAL ADVISORY COMMITTEE FOR AERONAUTICS, vol. REPORT NO 210.

[27] "Acanfora, M., De Marco, A., Lecce, L., Development of a Flight Dynamics Model of a Small Unmanned Airship. Proceedings of the The 58th CASI Aeronautics Conference - AERO 2011 , Montreal , Quebec, Canada, April 2011.".

[28] "E. A. Kulczycki, J. R. Johnson, On The Development of Parameterized Linear Analytical Longitudinal Airship Model, AIAA Guidance, Navigation And Control Conference And Exhibit, Paper No.7260, Honolulu (Hawaii), 2008.".

[29] i. M. Acanfora, "New Approach and Results on Stability and Control of Airship," PHD thesis, 2011.

[30] C. Rosema, J. Doyle, L. Auman, M. Underwood and W. B. Blake, "MISSILE DATCOM User's Manual - 2011 Revision," U.S. Army Aviation & Missile Research, Development and Engineering Center, pp. Control Design and Analysis Branch, Control Sciences Division, 2011.

[31] "B. L. Nagabhushan, Control Configuration of a Relaxed Stability Airship, Journal of Aircraft Vol. 28, No. 9, AIAA-46064-520, September 1991, pp. 558-563.".

[32] "F. Goineau and M. V. Cook, The stability and control characteristics of the neutrally buoyant non-rigid airship, College of Aeronautics Reports, Cranfield Institute of Technology, 1999.".

[33] "A. Kornienko, System Identification Approach for Determining Flight Dynamical Characteristics of an Airship from Flight Data, IFF, PhD Thesis, University of Stuttgart, August 2006.".

[34] "A. Moutinho, J. R. Azinheira, Stability and Robustness Analysis of the AURORA Airship Control System using Dynamic Inversion, Proceedings of the 2005 IEEE International Conference on Robotics and Automation Barcelona, Spain, April 2005, pp. 2265-2270.".

[35] "B. L. Nagabhushan, S. B. Tan, Directional Control of an Advanced Airship, Journal of Aircraft Vol. 33, No. 5, AIAA-47032-268, October 1996, pp. 895- 900.".

[36] C. F. D. Software, "http://www.ansys.com/Products/Fluids," last date accessed 1\8\2016. .

[37] M. V. Cook, K. G.A. and G. J.D., " Stability and Control. Chap. IV in Airship technology, Cambridge University Press,," 1999..

[38] J. NAKPIAM, "Control of Airship Motion in the Presence of Wind," University of Texas, 2011.

[39] "H. Wittrick, The Theory of Symmetrical Crossed Flexure Pivots , Australian Journal of Scientific Research, Series A: Physical Sciences, vol. 1, pp.121, 1948.".

[40] F. G. MARTINS, "TUNNING PID CONTROLLER USING ITAE CRITERION," Int. J. Engng, vol. 21, no. 5, pp. 867-873, 2005.

[41] A. O. Shuaib and M. M. Ahmed, "Robust PID Control System Design Using ITAE Performance Index," International Journal of Innovative Research in Science, Engineering and Technology, vol. 3, no. 7, 2014.

[42] "http://ctms.engin.umich.edu/CTMS/index.php?example=Introduction&section=ControlPID," last date accessed 1\8\2016. .

[43] R. C. Dorf and R. H. Bishop, "PID Controllers," in Modern Control Systems, PEARSON, 2007, pp. 391-393, 738-745.

[44] R. C. Dorf and R. H. Bishop, "The Design of State Variable Feedback Systems," in Modern Control Systems, PEARSON, 2007, pp. 659-722.

[45] last date accessed 1\8\2016. . Available: http://ctms.engin.umich.edu/CTMS/index.php?example=AircraftPitch&section=ControlStateSpace#2.

[46] R. KALMAN, "LECTURES ON CONTROLLABILITY AND OBSERVABILITY," Stanford University, California, 1970.

[47] F. Lewis, "Linear Quadratic Regulator (LQR) State Feedback Design," 2008.

[48] M.´ar and E. S.¨ohr, "Gain-scheduled LQR-control for an autonomous airship," in 18th International Conference on Process Control, Hagen, Germany, 2011.

[49] R. M. Murray, "Lecture 2 – LQR Control," CALIFORNIA INSTITUTE OF TECHNOLOGY Control and Dynamical Systems, California, 2006.

[50] B. Friedland, "FULL-ORDER STATE OBSERVER," department of electrical and computer engineering , New Jersey Institute of Technology, NEWARY, NEW JERSEY, USA.

[51] V. Radisavljevic-Gajic, "Linear Observers Design and Implementation," in Proceedings of 2014 Zone 1 Conference of the American Society for Engineering Education (ASEE Zone 1), 2014.

[52] J. L. D. A. Colozza, " High-Altitude, Long-Endurance Airships,," NASA Technical Memorandum, National Aeronautics and Space Administration,, John H. Glenn Research Center at Lewis Field Cleveland, Ohio, 2005.

[53] P. I. A. C. G. Andreutti, "Sintesi delle attività di aerodinamica," svolte dal CIRA sul progetto ZSFERA. CIRA (Italian Aerospace Research Centre), , 2009..

[54] "A. Colozza, J. L. Dolce, High-Altitude, Long-Endurance Airships, NASA Technical Memorandum, National Aeronautics and Space Administration, John H. Glenn Research Center at Lewis Field Cleveland, Ohio, 2005.".

[55] "G. Andreutti, P. Iannelli, A. Carozza, Sintesi delle attività di aerodinamica svolte dal CIRA sul progetto ZSFERA. CIRA (Italian Aerospace Research Centre), 2009.".

[56] "G. Kantor, D. Wettergreen, J. P. Ostrowski, S. Singh, Collection of Environmental Data From an Airship Platform. Proceedings of the SPIE Conference on Sensor Fusion and Decentralized Control IV. 2001. pp. 76-83.".

[57] "C. G. Justus, C. W. Campbell, M. K. Doubleday, D. L. Johnson, New Atmospheric Turbulence Model for Shuttle Applications. NASA Technical Memorandum 4168, NASA, 1990.".

[58] "J. R. Azinheira, E. Paiva, J. J. G. Ramos, S. S. Bueno, M. Bergerman, Extended Dynamic Model for AURORA Robotic Airship. AIAA Lighter-Than- Air Technology Conference, Akron, 2001.".

[59] "J. Rao, Z. Gong, Z. Xie, A Flight Control and Navigation System of a Small Size Unmanned Airship. IEEE International Conference on Mechatronics & Automation, Niagara Falls, Canada, 2005, pp. 1491-1496.".

[60] "L. G. B. Mirisola, J. Lobo, J. Dias, Stereo Vision 3D Map Registration for Airships. IASTED International Conference on Robotics and Applications (RA '06). Honolulu, Hawaii, 2006. pp. 102-107.".

[61] "M. Munk, The aerodynamic forces on airship hulls. NACA Report 184, NACA, 1924".

[62] "M. V. Cook , Stability and Control. Chap. IV in Airship technology, by Khoury G.A. and Gillett J.D., Cambridge University Press, 1999.".

[63] "S. B. V. Gomes, J. Jr. G. Ramos, Airship Dynamic Modeling for Autonomuos Operation. IEEE International Conference on Robotics & Automation, Leuven, Belgium, 1998, pp. 3462-3467.".

[64] "Y. J. Liang, G. Y. Tang, H. Ma, Optimal Control with Exponential Decay Rate for Offshore Platform Subjected to Irregular Wave Force. IEEE International Conference on Control and Automation, Xiamen, China, June 2010.".

[65] "M. V. Cook, The linearized small perturbation equations of motion for an airship, College of Aeronautics Reports, WP8, Cranfield Institute of Technology, 1990.".

[66] "N. La Gloria, Simultaneous localization and mapping applied to an airship with inertial navigation system and camera sensor fusion, CISAS, Phd Thesis, University of Padua , 2008.".

[67] "J. Roskam, Flight dynamics of rigid and elastic airplanes, Vol.1, Published by the author, Kansas City, USA, 1972, Chap. 4.".

[68] "L. Lecce and V. Gentile, Wind Tunnel Tests to Determine Longitudinal Dynamic Stability Derivatives on Models in Forced Oscillation , Proceedings of the V National Conference of the AIDAA, Milano, Italy, 26-29 Ott. 1979. Published on "Aerotecnica , Missili".

[69] "Principles of Naval Architects published by the Society of Naval Architects and Marine Engineers - SNAME.".

[70] "V. R. Cortes, J. R. Azinheira, E. C. Paiva, B. Faria, J. Ramos, S. Bueno, Experimental Identification of Aurora Airship, IAV2004 – 5th IFAC/EURON Symposium on Intelligent Autonomous Vehicles, Instituto Superior Técnico, Lisboa, Portugal July 2004.".

[71] "J. Kim, J. Keller, R. V. Kumer, Design and Verification of Controllers for Airships, Departmental Papers (MEAM), University of Pennsylvania, 2003.".

[72] "E. N. Goncalves, R. M. Palhares, R. H. C. Takahashi, H2/H1 Robust PID Synthesis for Uncertain Systems, Proceedings of the 45th IEEE Conference on Decision & Control, San Diego, CA, USA, December 2006, pp. 4375-4380.".

[73] "P. G. Thomasson, equations of Motion of a Vehicle in a Moving Fluid, Journal of Aircraft Vol. 37, No. 4, AIAA-2645-634, August 2000, pp.630- 639.".

[74] "Y. Li, M. Nahon, Modeling and Simulation of Airship Dynamics, Journal of Guidance Control and Dynamics, Vol. 30, No. 6, AIAA-29061-200,December 2007, pp. 1691-1700.".

[75] "B. L. Nagabhushan, Dynamic Stability of a Buoyant Quad-Rotor Aircraft, Journal of Aircraft, Vol. 20, No. 3, AIAA-44859-486, March 1983, pp. 243- 249.".

[76] "N. E. Leonard, J. G. Graver, Model-Based Feedback Control of Autonomous Underwater Gliders, IEEE Journal of Oceanic Engineering, Vol. 26, No. 4, October 2001, pp. 633-645.".

[77] "B. H. Beheshti, F. Wittmer, R. S. Abhari, Flow visualization study of an airship model using a water towing tank, Aerospace Science and Technology, August 2009, pp. 450-458.".

[78] "L. Valera, B. L. Nagabhushan, Design Trends and Global Developments in Modern Lta Vehicles, ICAS Congress, 2002.".

[79] "T. Lutz, P. Funk, A. Jakobi, S. Wagner, Summary of Aerodynamic Studies on the Lotte Airship, 4th International Airship Convention and Exhibition, Cambridge, England, July 2002.".

[80] "T. Lutz, P. Funk, A. Jakobi, S. Wagner, Aerodynamic Investigations on Inclined Airship Bodies, 2th International Airship Convention and Exhibition, Bedford, Great Britain, June 1998.".

[81] "M. Acanfora, A. De Marco, L. Lecce, Development, Modeling and Simulation of Multiple Design Concepts for a Small Unmanned Airship, Proceedings of the AIAA Modeling and Simulation Technology Conference, Portland, Oregon, USA, AIAA-MST 2011-6521-967, August".

[82] "M. Acanfora, A. De Marco, L. Lecce, Stability and Control Analysis for a Non-Rigid Unmanned Airship with Different Tail Configurations, Proceedings of the Specialists Meeting NATO AVT-189/RSM-028, Portsdown West, UK, October 2011.".

[83] "AM. Acanfora, L. Lecce, On the Development of the Linear Longitudinal Model for Airship's Stability in Heaviness Condition, Accepted on "Aerotecnica Missili e Spazio" 07/09/2011.".

[84] "http://blog.opticontrols.com/archives/884," last date accessed 1\8\2016. .